International Journal of Recent Technology and Engineering (IJRTE)
ISSN: 2277-3878, Volume-8 Issue-4, November 2019

# The Effect of Slat Opening on Vortex Shedding Behind a Circular Cylinder

**M.R.A. Misman, A.M. Azmi, Z.A. Kamarulbaharin, A.H.A. Hamid**

***Abstract:*** ***Add-on devices are widely used as one of the means of suppressing vortex induced vibrations from bluff bodies. The present study numerically investigates flow over a circular cylinder attached by an axial slat. The axial slat were of uniform and non-uniform openings of 67% and 44% porosity. The governing equation was solved using viscous-laminar model at Reynolds number, Re=300. It was found that the presence of the axial slats significantly suppressed vortex shedding behind the circular cylinder. The non-uniform slats showed longer vortex formation length with lower drag, in comparison to that of the uniform slats. In addition, the slats with 67% porosity of both uniform and non-uniform openings suppressed vortex better than that of 44% porosity slats, indicated by the longer vortex formation length and weaker intensity of vortices.***

***Keywords: axial slat, shroud, vortex shedding, VIV.***

## I. INTRODUCTION

Flow around a circular cylinder has been the subject of numerous studies particularly in fundamental fluids mechanics problem. It has potential relevance for practical application in engineering such as submarines and bridges. The vortex shedding in the wake region produces from such flow could cause acoustic noise, vibration, fatigue and shortens the life of the cylinder. It is important to control the flow to avoid unwanted problems in the structural designs.

In fluid mechanics, flow around a circular cylinder has been the focus of many studies and is relevant in real-world engineering applications such as bridges and submarines. The wake region generates vortex shedding and this may trigger acoustic noise, vibration, fatigue and shorten the life of the cylinder. Therefore, in structural designs, it is central to control the flow to avoid undesirable complications.

Manuscript published on November 30, 2019.
* Correspondence Author
**Muhammad Rafiq Adha Misman***, Faculty of Mechanical Engineering, Universiti Teknologi MARA, Shah Alam, Malaysia. Email: rafiqmisman00@gmail.com
**Azlin Mohd Azmi***, Faculty of Mechanical Engineering, Universiti Teknologi MARA, Shah Alam, Malaysia. Email: azlinazmi@uitm.edu.my
**Zainal Abidin Kamarul Baharin**, Faculty of Mechanical Engineering, Universiti Teknologi MARA, Shah Alam, Malaysia. Email: zainalkb@uitm.edu.my
**Ahmed Hussein Abdul Hamid**, Faculty of Mechanical Engineering, Universiti Teknologi MARA, Shah Alam, Malaysia. Email: hussein@uitm.edu.my



Suppression of vortices may be carried out via passive or active flow control methods. Inhibiting the occurrence of vortex shedding along the length of the structure or the formation of the wake vortices and their interactions can be done by altering the structural profile [1]. In addition, vibration suppression may also be achieved through the

concept of base bleed as showcased in the work of Price [2] using perforated shrouds. Boorsma [3] discovered that the low frequency noise introduced by solid fairings on landing gear models can be reduced by replacing them with perforated fairings. Ikeda and Takaishi [4] disclosed that the jets emitted from holes of their perforated cylinder at regular intervals displayed stable wake shear layers and suppression of Aeolian tone. Zhao and Cheng [5] verified that suitable selection a porous material will reduce the lift of circular cylinder. An experimental study by Kleissl and Georgakis [6] on a bridge cable showed that vortex-induced oscillating lift forces is significantly reduced with a shroud cylinder. A numerical study by Yu et al [7] on steady flow around a porous circular cylinder disclosed that contrary to a solid cylinder, a recirculating wake develops downstream of or within the cylinder but not from the surface. Using the penalization method, Bruneau and Mortazavi [8, 9] learnt that vortex induced vibrations can be damped by adding a porous ring around the riser pipe. Experimental work on the control of vortical flow of circular cylinder using a splitter plate having different lengths and heights was carried out by Gozmen et.al [10]. The results of the study by Pinar et al [11] on flow structure of perforated cylinder in shallow water revealed that porosity has a significant effect on the control of large-scale vortical structures downstream of a cylinder. An experiment by Sahin [12] using perforated plate as a flow control device ascertained that non-uniformity in the velocity is increase as the porosity is decreased.

An axial slat is one of the shroud examples other than the perforated shrouds, with thin narrow flat strips and slots in between strips. However, not many studies are done on this body despites its simple geometry. The present study attempts to enhance the effectiveness of the slats as an add-on device through non-uniform slots or opening by studying the flow over the coupled slat-cylinder body at Reynolds number of 300.

## II. METHODOLOGY

The study of two-dimensional CFD simulation was first done by validating the simulation of flow over cylinder with the existing studies to confirm the simulation setup and get a credible model.

The mean drag coefficient, $C_d$ and Strouhal number, St were compared with the experimental and numerical results, as reported in Table I. The present numerical value of the drag coefficient and Strouhal agree reasonably well with each corresponding values of literatures, with a difference of about less than 10% and 7%, respectively.

The geometrical setup and computational domain is presented in Fig. 1. The flow was set to be two-dimensional. The diameter of the circular cylinder ($d$) was 1 m. The diameter ratio of the slatted cylinder to the circular cylinder ($D/d$) was fixed at 2. The domain extent 10$d$ and 40$d$ upstream and downstream of the cylinder, respectively. The top and bottom boundaries were both located at 20d from the cylinder axis. The wall and cylinder setup was stationary wall boundary and no-slip condition, respectively.

**Table -I: Drag Coefficient and Strouhal Number**

| Shape | | $C_d$ | St |
|---|---|---|---|
| Circular Cylinder | B.N Rajani (2005) [13] | 1.37 | 0.2150 |
| | Mittal & Balachandar (1997) [14] | 1.38 | 0.213 |
| | Present study | 1.34 | 0.200 |
| | Experiment [15] | 1.22 | - |
| | Experiment [16] | - | 0.203 |
| 67% Slatted cylinder | Uniform slat opening | 1.17 | 0.060 |
| | Non-Uniform slat opening | 1.12 | 0.060 |
| 44% Slatted Cylinder | Uniform slat opening | 1.21 | 0.065 |
| | Non –Uniform slat opening | 1.15 | 0.065 |

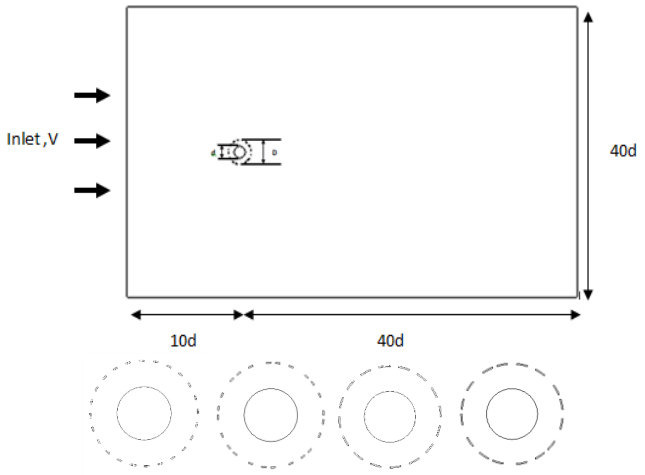


**Fig. 1. Computational domain and slat geometry of 67% porosity (uniform and non-uniform holes) and 44% porosity (uniform and non-uniform holes)**

The geometry of 67% and 44% slatted cylinders was shown in Fig. 1 respectively. The opening or porosity, $\beta$ of the axial slat is defined as follows:

$$\beta = \frac{ns}{\pi D} \quad (1)$$

where $n$ is number of opening and $s$ is the arc length of one opening ($s=(D/2)\,\theta$). The angle, θ defines the opening size and $\theta = \pi/18 = 10°$ was set for the uniform slat opening. Therefore, $\beta = \frac{ns}{\pi D} = \frac{n.(D/2)(\pi/18)}{\pi D} = n/36$; where $n$=24 and 16 for $\beta$= 67% and 44% respectively.

For the non-uniform opening, three different values of $\theta$ were used, i.e. θ=5°, 10° and 15° where each angle was assigned to different numbers of opening, depending on the porosity. The general equation to calculate the porosity for non-uniform opening is:

$$\beta = \frac{(p \times s1) + (q \times s2) + (r \times s3)}{\pi D} \quad (2)$$

where s1, s2 and s3; and p, q and r; are the arc length and number of opening representing $5°, 10°, 15°$ opening size respectively. For $\beta$ = 0.44 the value of ($p$, $q$, $r$) = (2, 4, 2) and for $\beta$ = 0.67, ($p$, $q$, $r$) = (4, 4, 4).

Mesh structure is important in order to get accurate and credible result. Fig. 2 shows the mesh structure using structured meshing.

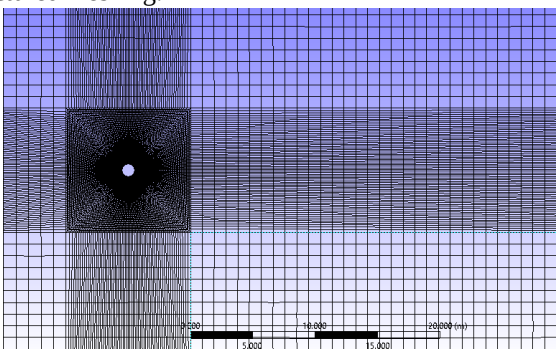

**Fig. 2. Structured meshing**

**Table -II: Grid information**

| Geometry | Grid | $C_d$ | St |
|---|---|---|---|
| 67% Slatted Cylinder (Uniform slat) | Coarse | 1.11 | 0.055 |
| | Medium | 1.15 | 0.060 |
| | Fine | 1.17 | 0.060 |
| | Superfine | 1.18 | 0.060 |
| 67% Slatted Cylinder (Non-Uniform Slat) | Coarse | 1.09 | 0.060 |
| | Medium | 1.10 | 0.060 |
| | Fine | 1.12 | 0.060 |
| | Superfine | 1.12 | 0.060 |
| 44% Slatted Cylinder (Uniform Slat) | Coarse | 1.17 | 0.065 |
| | Medium | 1.19 | 0.065 |
| | Fine | 1.21 | 0.065 |
| | Superfine | 1.21 | 0.065 |
| 44% Slatted Cylinder (Non-Uniform Slat) | Coarse | 1.14 | 0.060 |
| | Medium | 1.15 | 0.065 |
| | Fine | 1.15 | 0.065 |
| | Superfine | 1.17 | 0.065 |

The model used in this study was viscous laminar model in transient time to simulate unsteady flow at $Re$=ρV$d$/μ=300, where V is the incoming velocity. A second order implicit solution method was used in the computational simulation

for better accuracy. The simulation was initialized by hybrid initialization where the calculation was run at time step size of 0.001s for 1500 number of time step with 50 maximum iterations per time step.

Grid independence study was performed to increase the numerical accuracy of computational results and the influence of the number of grid size as shown in Table II. The study was done by increasing the numbers of cells and nodes of the mesh which are fine, medium and coarse meshing. The fine mesh was sufficient to be used for the simulations.

## III. RESULTS AND DISCUSSION

Fig. 3,4,5,6, and 7 show the time history of lift and drag coefficients, $C_l$ and $C_d$ for the circular cylinder and slatted cylinder respectively. It can be seen clearly the periodic nature of the flow in the circular cylinder due to the presence of correlated vortex shedding. However, for the slatted cylinders, the oscillation are significantly suppressed indicating low correlation of vortex especially for that of 67% porosity slatted cylinder, with an order less than one tenth magnitude in comparison to that of 44% porosity. The value of drag coefficient of the slatted cylinders reduced significantly, about 17% reduction than that of the circular cylinder case. The uniform slats have a slightly higher drag coefficient than that of non-uniform slats for both porosity values.

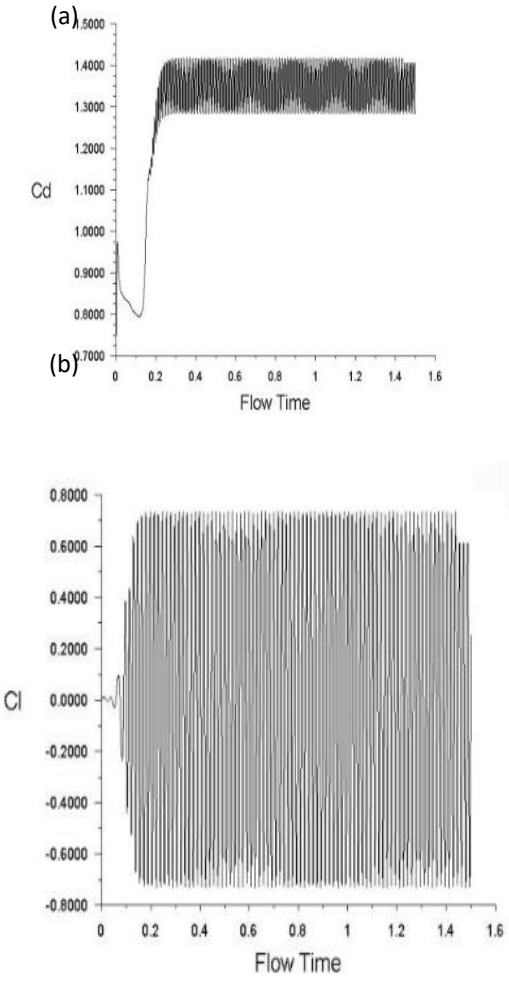


**Fig. 3. (a) Time history of Drag coefficient (b) Time history of Lift coefficient for circular cylinder at *Re*=300.**

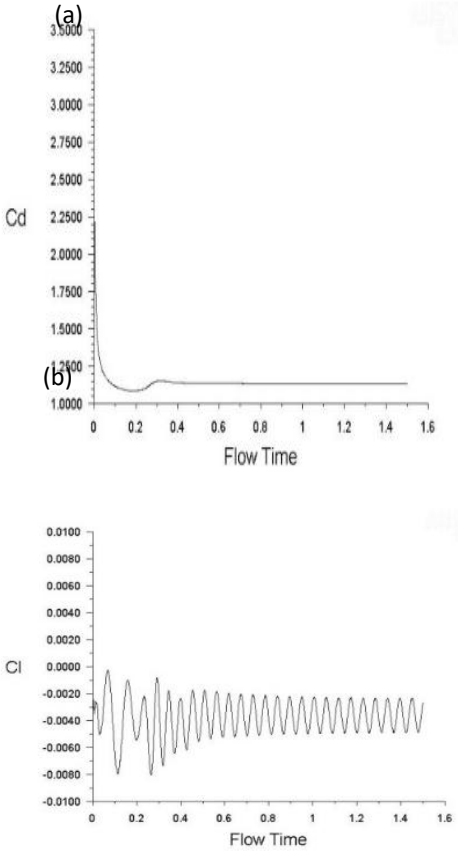


**Fig. 4. (a) Time history of Drag coefficient (b) Time history of Lift coefficient for 67% uniform of slatted cylinder at *Re*=300.**

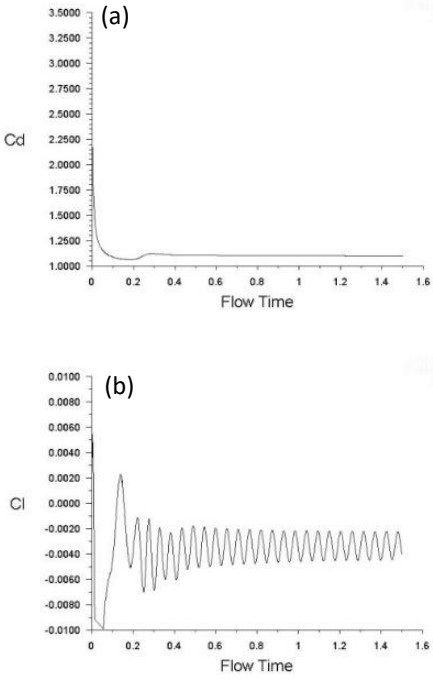


**Fig. 5. (a) Time history of Drag coefficient (b) Time history of Lift coefficient for 67% non-uniform of slatted cylinder at *Re*=300.**

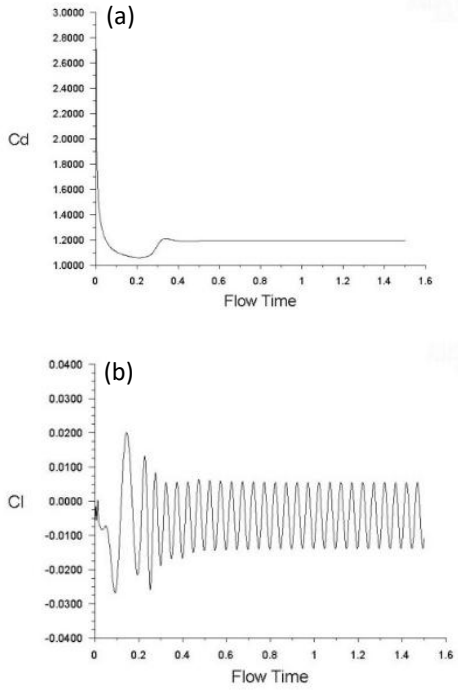


**Fig. 6. (a) Time history of Drag coefficient (b) Time history of Lift coefficient for 44% uniform of slatted cylinder at *Re*=300.**

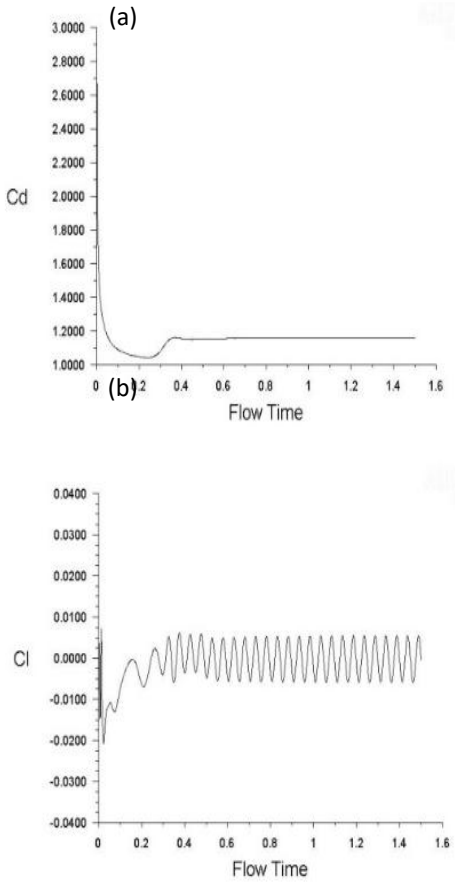


**Fig. 7. (a) Time history of Drag coefficient (b) Time history of Lift coefficient for 44% non-uniform of slatted cylinder at *Re*=300.**

Fig. 8, 9, and 10 show the power spectral density of lift coefficient of the circular cylinder and slatted cylinders, respectively. From the observation, the magnitude of power spectral density for a circular cylinder is significantly reduced with the addition of the slatted cylinders, with the most reduction achieved by the 67% non-uniform slats. The Strouhal number corresponding to the main shedding frequency is obtained from the maximum peak where for the slatted cylinders, they are in the range of 0.06 and 0.065 compare to the circular cylinder of 0.2.

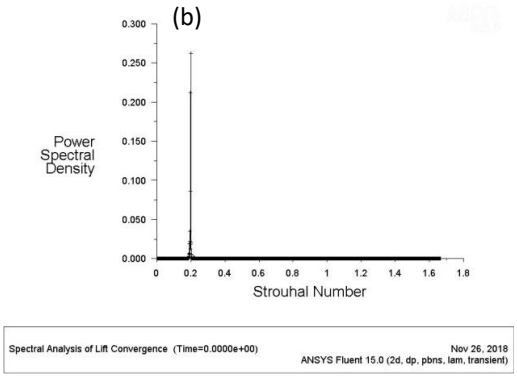


**Fig. 8. Strouhal number for circular cylinder**

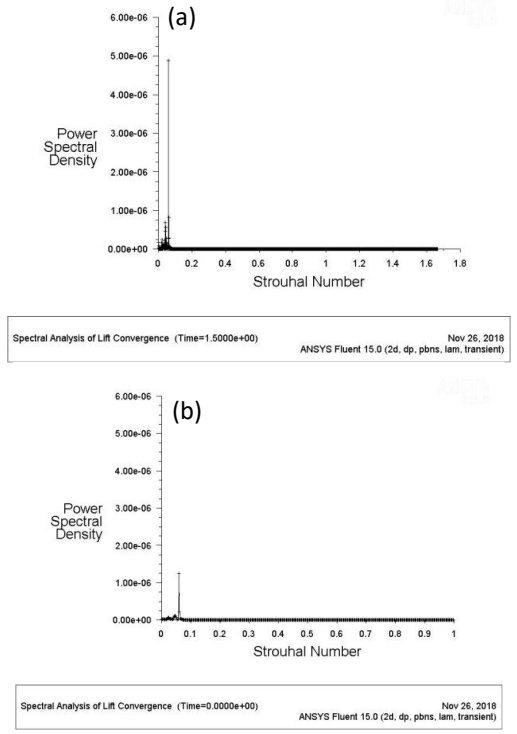


**Fig. 9. Strouhal number of (a) 67% uniform (b) 67% non-uniform for slatted cylinder**

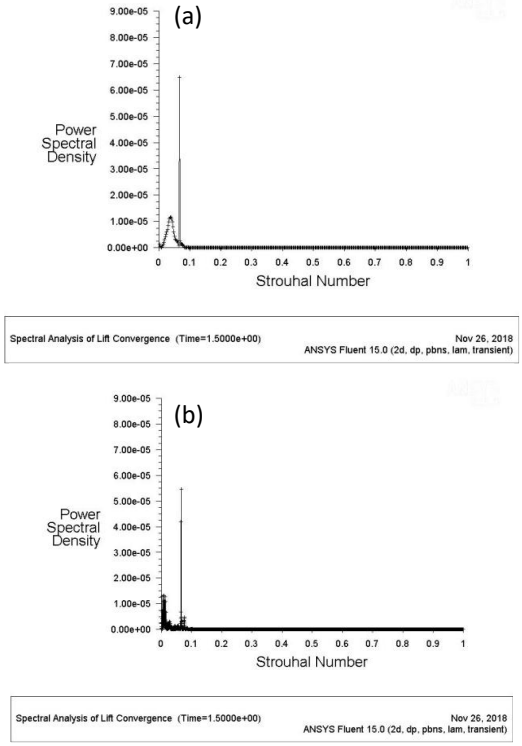


**Fig. 10. Strouhal number of (a) 44% uniform (b) 44% non-uniform for slatted cylinder**

Fig. 11, 12, and 13 show the pressure coefficient contour for all cylinders. The low pressure region is indicated by the blue colour where vortices form closer to the circular cylinder in comparison to that of the slatted cylinders where the low pressure regions are not observed immediately behind their wakes, particularly that of 67% porosity.

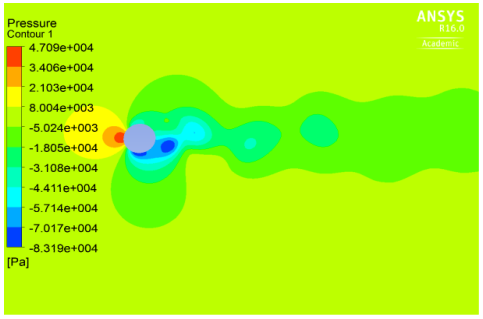


**Fig. 11. Pressure coefficient contour for circular cylinder**

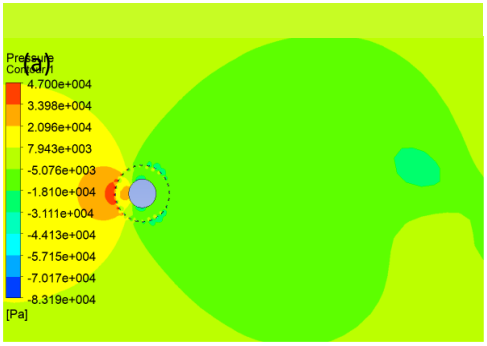


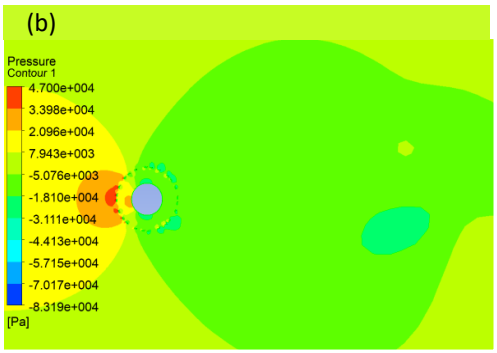


**Fig. 12. Pressure coefficient contour (a) 67% uniform (b) 67% non-uniform for slatted cylinder**

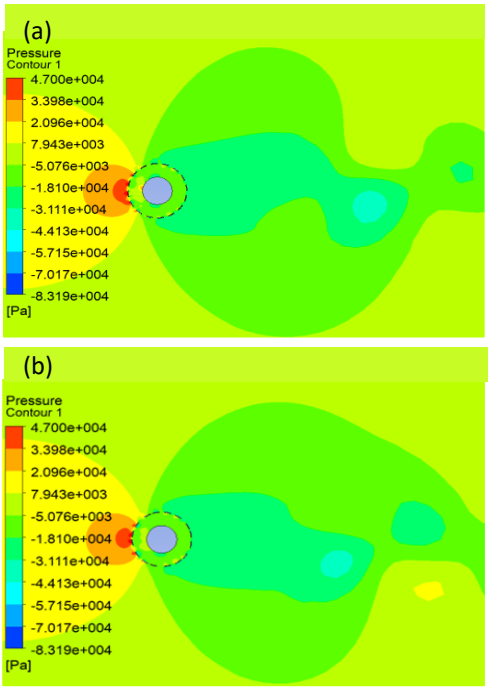


**Fig. 13. Pressure coefficient contour (a) 67% uniform (b) 67% non-uniform for slatted cylinder**

Fig. 14,15,16,17, and 18 show the velocity and vorticity contours for all cylinders respectively. The slatted cylinders significantly suppress the vortex shedding from a circular cylinder. The stagnation point can be seen in front of the circular cylinder and the slatted cylinders. However, the flow passes through the slats opening with moderate velocity in the annular region, and becomes zero at the central wake region of all slatted cylinders. This low velocity region is formed farther in the slatted cylinder wakes of high porosity (67%) compared to that of low porosity (44%) of both uniform and non-uniform slat openings. In the normalized vorticity contour, the red colour indicates clockwise vorticity and blue colour signifies counter clockwise vorticity. The high intensity Karman vortices occurs immediately behind the circular cylinder while low intensity small vortices occur within the annular region of the slatted cylinders and extend in the shear layers. A Karman-like vortices of fairly low intensity are only observed later in the wake of the slatted cylinders, where the formation length is longer for the high porosity 67% cylinder than that in the 44% porosity cylinder.

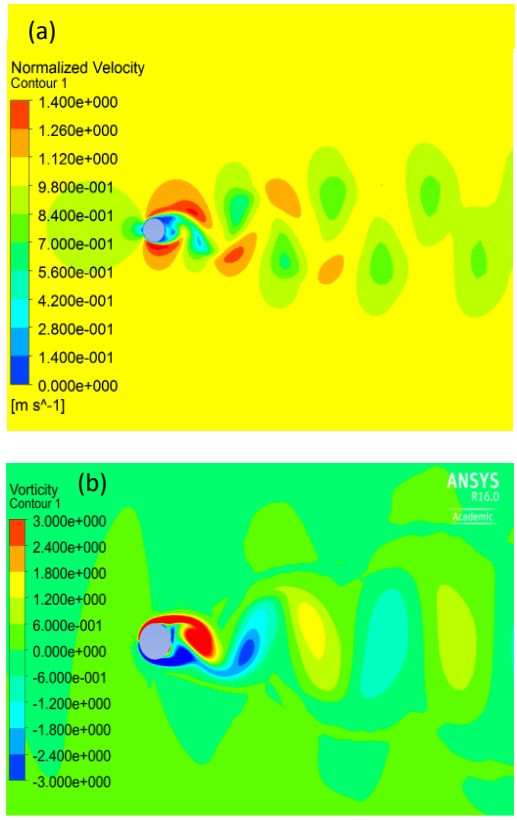


**Fig. 14. (a) Normalize velocity contour (b) vorticity contour for circular cylinder**

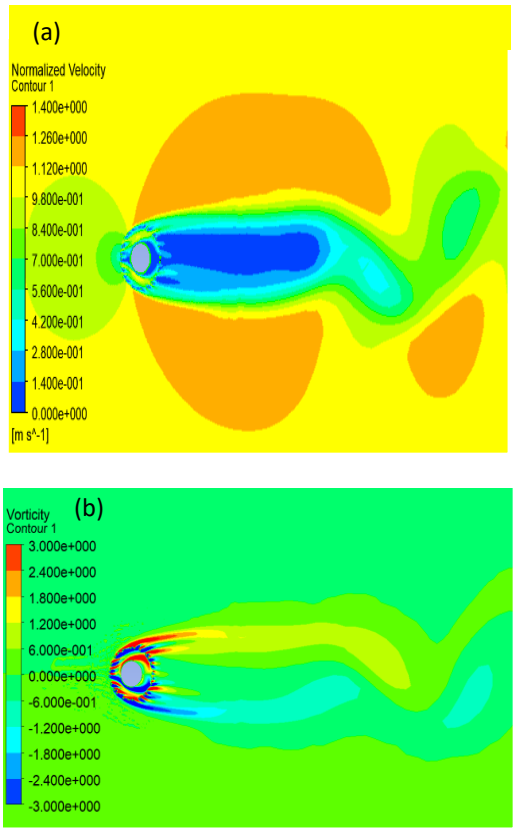


**Fig. 16. (a) Normalize velocity contour (b) vorticity contour for 67% non-uniform slatted cylinder**

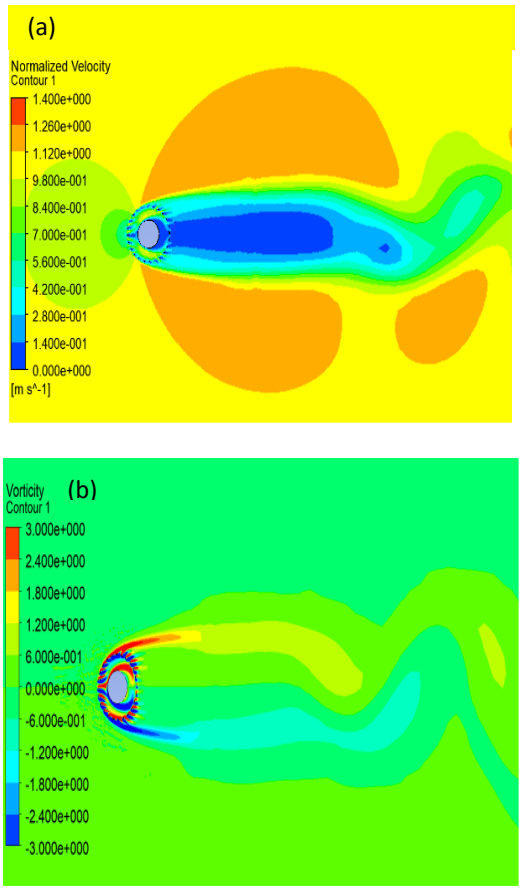


**Fig. 15. (a) Normalize velocity contour (b) vorticity contour for 67% uniform slatted cylinder**

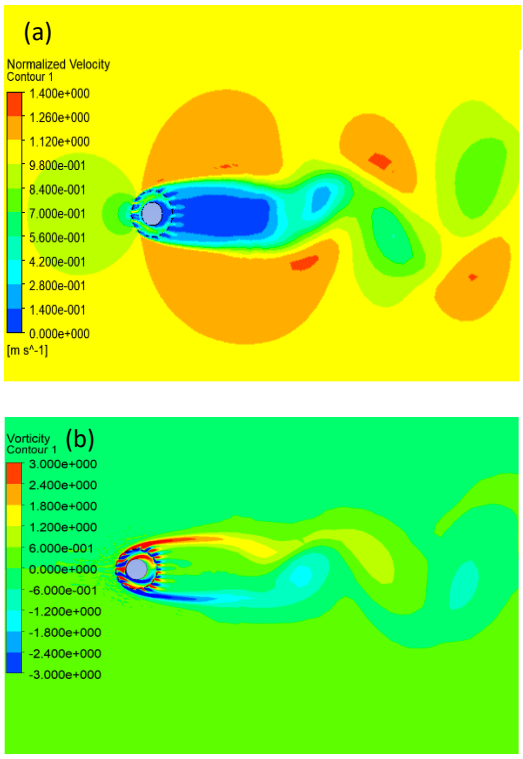


**Fig. 17. (a) Normalize velocity contour (b) vorticity contour for 44% uniform slatted cylinder**

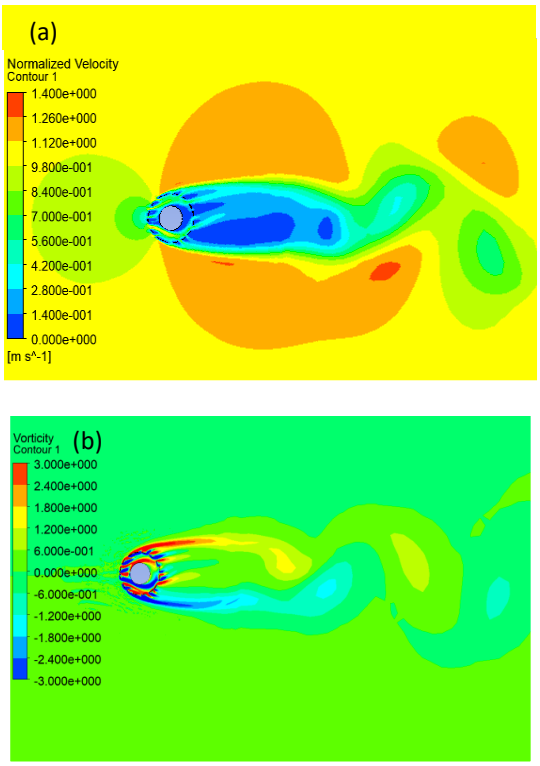


**Fig. 18. (a) Normalize velocity contour (b) vorticity contour for 44% non-uniform slatted cylinder**

## IV. CONCLUSION

The effects of axial slats on the wake behind a circular cylinder was numerically investigated at *Re*=300. The slats were of 67% and 44% porosity with uniform and non-uniform openings. The simulations revealed that the presence of the slats significantly affected the flow region behind the circular cylinder. In terms of drag reduction, the non-uniform slats gave lower drag in comparison to the uniform slats for both porosities. In addition, high porosity slats showed better drag reduction in comparison to the low porosity slat with the exception of non-uniform slats of 44%. The magnitude of power spectral density was also reduced significantly using the non-uniform slats and high porosity slats. Pressure, velocity and vorticity contours also showed better vortex suppression effect of the non-uniform and high porosity slats with longer vortex formation length and elongated low velocity region observed from the contours in comparison to that of uniform slats and low porosity slats. This study could be extended to three dimensional flow and at high Reynolds numbers.

## REFERENCES

1. M.J. Every, R. King, D.S. Weaver., "Vortex-excited vibrations of cylinders and cables and their suppression", Ocean Engineering, vol. 9, pp. 135-157, 1982.
2. P. Price, "Suppression of the fluid-induced vibration of circular cylinders," J. Eng. Mech. Div., Am. Soc. Civ. Eng., vol. 82, pp. 1030, 1956.
3. K. Boorsma, X. Zhang, N. Molin, L. C. Chow, "Bluff body noise control using perforated fairings," AIAA J., vol. 47, pp. 33-43, 2009.
4. M. Ikeda, T. Takaishi, "Perforated pantograph horn aeolian tone suppression mechanism, " Q. Report of RTRI (Jpn), vol. 45, pp. 169-174, 2004.
5. M. Zhao, L. Cheng, "Finite element analysis of flow control using porous media," Ocean Eng., vol. 37, pp. 1357- 1366, 2010.
6. K. Kleissl, C. T. Georgakis, "Aerodynamic control of bridge cables through shape modification: A preliminary study," J. Fluids Struc. 27, pp. 1006-1020, 2011.
7. P. Yu, Y. Zeng, T. S. Lee, X. B. Chen, H. T. Low, "Steady flow around and through a permeable circular cylinder," Comp. Fluids, vol. 42, pp. 1-12, 2011.
8. C-H Bruneau, I. Mortazavi, "Passive control of the flow around square cylinder using porous media," International Journal for Numerical Methods in Fluids, vol. 45, pp. 415–433, 2004.
9. C-H Bruneau, I. Mortazavi, "Numerical modelling and passive flow control using porous media," Computers and Fluids, vol. 37, pp. 488–498, 2008.
10. B. Gozmen, H. Akilli, B. Sahin, "Passive control of circular cylinder wake in shallow flow," Measurement, vol. 46, pp. 1125-1136, 2013.
11. E. Pinar, G.M. Ozkan, T. Durhasan, M.M. Aksoy, H. Akilli, B. Sahin, "Flow structure around perforated cylinders in shallow water," Journal of Fluids and Structure, vol. 55, pp. 52-63, 2015.
12. B. Sahin, "Pressure losses in an isolated perforated plate and jets emerging from the perforated plate," International Journal of Mechanical Science, vol. 31, pp. 51-61, 1989.
13. B.N. Rajani, H.S. Lanka, and S. Majumdar, "Laminar flow past a circular cylinder at reynolds number varying from 50 to 5000," NAL PD CF 0501, (2005)
14. R. Mittal, S. Balachandar, "On the inclusion of three-dimensional effects in simulations of two-dimensional bluff body wake flows," Proc. of the ASME Fluids Eng. Div. Summer Meetg.(Vancouver), (1997)
15. C. Wieselsberger, "New data on the law of hydro and aerodynamic resistance" NACA TN 84, 1992
16. C.H.K. Williamson, "Vortex dynamics in the cylinder wakes," Ann. Rev. Fluid Mech., vol. 28, pp. 477-539, 1996.

## AUTHORS PROFILE

**Muhammad Rafiq Adha Misman** completed his Bachelor Degree (Hons.) in Mechanical Engineering from Universiti Teknologi MARA in 2018.

**Azlin Mohd Azmi** is currently serving as Senior Lecturer at the Faculty of Mechanical Engineering, Universiti Teknologi MARA. She received her Bachelor Degree in Mechanical Engineering from Universiti Teknologi MARA and M.Eng from University of Adelaide. She obtained her Ph.D from University of Western Australia. She is an associate member of the Energy Institute, U.K and a Certified Carbon Reduction Manager (CRM). Her research interests include flow-induced vibration suppression and enhancement as well as energy and carbon footprint.

**Zainal Abidin Kamarul Baharin** is currently a Senior Lecturer at the Faculty of Mechanical Engineering, Universiti Teknologi MARA. He received his Bachelor Degree in Mechanical Engineering from Louisiana State University, USA and his MSc. from Fachhochschule Karlsruhe, Germany. He is a licensed professional engineer in the USA and a registered professional engineer in Malaysia. His research interests include solar still, solar pond and biofuel.

**Ahmad Hussein Abdul Hamid** is a Senior Lecturer at the Faculty of Mechanical Engineering, Universiti Teknologi MARA, Malaysia. He received his M.Sc. degree in 2008 from the same university. In 2016, He obtained his PhD in Mechanical Engineering from Monash University, Melbourne and specializes in the field of magnetohydrodynamics and heat transfer. His research interests include wake flow of a bluff body, magnetohydrodynamic flow, heat transfer, liquid atomization and renewable energy.